

Optical tweezers with millikelvin precision of temperature-controlled objectives and base-pair resolution

Mohammed Mahamdeh¹ and Erik Schäffer^{1,*}

¹*Nanomechanics Group, Biotechnology Center, TU Dresden, Tatzberg 47-51, 01307 Dresden, Germany*

Erik.Schaeffer@biotec.tu-dresden.de

Abstract: In optical tweezers, thermal drift is detrimental for high-resolution measurements. In particular, absorption of the trapping laser light by the microscope objective that focuses the beam leads to heating of the objective and subsequent drift. This entails long equilibration times which may limit sensitive biophysical assays. Here, we introduce an objective temperature feedback system for minimizing thermal drift. We measured that the infrared laser heated the objective by 0.7 K per watt of laser power and that the laser focus moved relative to the sample by ≈ 1 nm/mK due to thermal expansion of the objective. The feedback stabilized the temperature of the trapping objective with millikelvin precision. This enhanced the long-term temperature stability and significantly reduced the settling time of the instrument to about 100 s after a temperature disturbance while preserving single DNA base-pair resolution of surface-coupled assays. Minimizing systematic temperature changes of the objective and concurrent drift is of interest for other high-resolution microscopy techniques. Furthermore, temperature control is often a desirable parameter in biophysical experiments.

© 2009 Optical Society of America

OCIS codes: (000.2170) Equipment and techniques; (120.6780) Temperature; (140.7010) Laser trapping; (140.6810) Thermal effects; (170.0180) Microscopy; (350.4855) Optical tweezers or optical manipulation;

References and links

1. W. Denk and W. W. Webb, "Optical measurement of picometer displacements of transparent microscopic objects," *Appl. Opt.* **29**, 2382–2391 (1990).
2. E. A. Abbondanzieri, W. J. Greenleaf, J. W. Shaevitz, R. Landick, and S. M. Block, "Direct observation of base-pair stepping by RNA polymerase," *Nature* **438**, 460–465 (2005).
3. W. J. Greenleaf, M. T. Woodside, and S. M. Block, "High-resolution, single-molecule measurements of biomolecular motion," *Annu. Rev. Biophys. Biomol. Struct.* **36**, 171–190 (2007).
4. J. R. Moffitt, Y. R. Chemla, K. Aathavan, S. Grimes, P. J. Jardine, D. L. Anderson, and C. Bustamante, "Inter-subunit coordination in a homomeric ring ATPase," *Nature* **457**, 446–450 (2009).
5. A. R. Carter, G. M. King, T. A. Ulrich, W. Halsey, D. Alchenberger, and T. T. Perkins, "Stabilization of an optical microscope to 0.1 nm in three dimensions," *Appl. Opt.* **46**, 421–427 (2007).
6. E. Schäffer, S. F. Nørrelykke, and J. Howard, "Surface forces and drag coefficients of microspheres near a plane surface measured with optical tweezers," *Langmuir* **23**, 3654–3665 (2007).
7. M. D. Wang, H. Yin, R. Landick, J. Gelles, and S. M. Block, "Stretching DNA with optical tweezers," *Biophys. J.* **72**, 1335–1346 (1997).

8. K. Neuman and S. Block, "Optical Trapping," *Rev. Sci. Instrum.* **75**, 2787–2809 (2004).
 9. K. Svoboda and S. M. Block, "Biological Applications of Optical Forces," *Annu. Rev. Biophys. Biomol. Struct.* **23**, 247–285 (1994).
 10. H. B. Mao, J. R. Arias-Gonzalez, S. B. Smith, I. Tinoco, and C. Bustamante, "Temperature control methods in a laser tweezers system," *Biophys. J.* **89**, 1308–1316 (2005).
 11. E. Fällman and O. Axner, "Design for fully steerable dual-trap optical tweezers," *Appl. Opt.* **36**, 2107–2113 (1997).
 12. V. Bormuth, J. Howard, and E. Schäffer, "LED illumination for video-enhanced DIC imaging of single microtubules," *J. Microsc.* **226**, 1–5 (2007).
 13. A. Pralle, M. Prummer, E. L. Florin, E. H. K. Stelzer, and J. K. H. Hörber, "Three-dimensional high-resolution particle tracking for optical tweezers by forward scattered light," *Microsc. Res. Tech.* **44**, 378–386 (1999).
 14. S. F. Tolić-Nørrelykke, E. Schäffer, J. Howard, F. S. Pavone, F. Jülicher, and H. Flyvbjerg, "Calibration of optical tweezers with positional detection in the back focal plane," *Rev. Sci. Instrum.* **77**, 103,101 (2006).
 15. G. M. Gibson, J. Leach, S. Keen, A. J. Wright, and M. J. Padgett, "Measuring the accuracy of particle position and force in optical tweezers using high-speed video microscopy," *Opt. Express* **16**, 14,561–14,570 (2008).
 16. A. R. Carter, Y. Seol, and T. T. Perkins, "Precision Surface-Coupled Optical-Trapping Assay with One-Basepair Resolution," *Biophys. J.* **96**, 2926–2934 (2009).
 17. S. W. Hell and J. Wichmann, "Breaking the diffraction resolution limit by stimulated-emission—stimulated-emission-depletion fluorescence microscopy," *Opt. Lett.* **19**, 780–782 (1994).
-

1. Introduction

Optical tweezers with back-focal-plane detection have picometer precision on time scales shorter than ≈ 1 ms [1]. In contrast, on time scales longer than ≈ 1 s, nanometer movements are often caused by instrumental noise in particular thermal drift. To achieve sub-nm resolution on long time scales for high-resolution measurements of DNA-protein interactions, differential measurements have been developed either in form of dual-trap assays decoupled from surfaces [2–4] or by active tracking of a fiducial mark for surface-coupled assays [5]. Differential measurements reduce noise because drift affects both recorded positions nearly equally and can thus be subtracted. Absolute measurements of surface-coupled assays have achieved sub-nm resolution by employing a simple, mechanically stable instrument and minimizing laser intensity fluctuations and pointing stability [6].

Experimental procedures during trapping assays involve changes in laser intensity, for example, in form of closing a shutter to trap a new particle or due to changes in trap stiffness [7, 8]. For infrared lasers, such intensity changes lead to a significant change in heating of the trapping objective [9]. Since thermal relaxation times of the objective and more importantly its mount are on the order of several 100–1000 s—as we will show below—long equilibration times are needed to regain stable conditions. Such long times are often not desirable in sensitive single molecule biophysical assays. To reduce equilibration times, active temperature stabilization is necessary. Commercially available objective heaters provide temperature stability to within 0.1 K at best. Objective heating by fluid-pumped copper jackets reached similar temperature stability [10]. Such a temperature range leads to approximately 100 nm expansion of an objective based on a linear thermal expansion coefficient of $\approx 20 \cdot 10^{-6} \text{ K}^{-1}$ and an objective size of ≈ 5 cm. This expansion directly shifts the focal point of the objective relative to the sample and therefore leads to drift of the optical tweezers relative to the surface. Thus, to achieve nm-resolution for absolute measurements, the objective temperature needs to be stabilized with millikelvin precision.

Here, we implement an objective temperature heating system based on Pt100 resistance temperature detectors and heating foils which are controlled via custom-written software using LabVIEW. We achieve millikelvin precision with about 8 s response time of the temperature feedback. By tracking immobilized microspheres on surfaces, we demonstrate the overall performance of the feedback and the detrimental heating effects that the laser has.

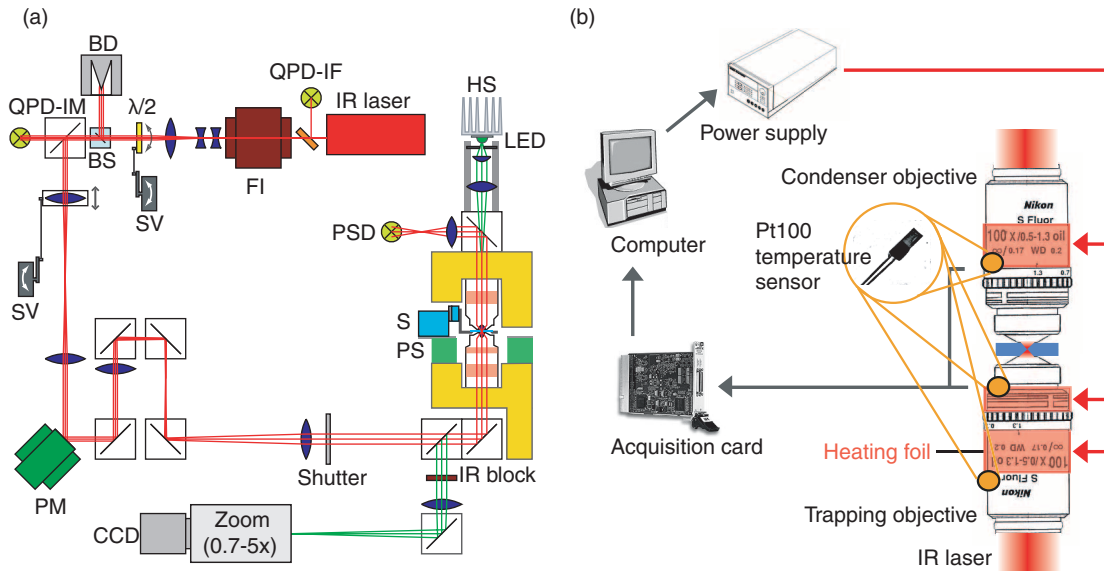


Fig. 1. (a) Schematic drawing of the optical tweezers apparatus. QPD-IF, quadrant photo-diode for intensity feedback; FI, Faraday isolator; $\lambda/2$, half-wave plate; SV, servo; BS, beam splitter; BD, beam dump; QPD-IM, quadrant photo-diode for intensity monitoring; PM, piezo mirror; PS, piezo translation stage; S, stage; PSD, position sensitive diode; LED, light emitting diode; HS, heat sink. The self-made inverted microscope (yellow) on the right-hand side is drawn as a side view, the remaining setup as a top view. (b) Schematic drawing of the temperature feedback. The red bands around the objectives indicate approximately the position and size of the heating foils.

2. Materials and methods

2.1. A compact & stable optical tweezers setup

The compact optical tweezers [Fig. 1(a)] were built on an active vibration isolation system (60 Basic, Halcyonics, Göttingen, Germany) employing a $80 \times 100 \text{ cm}^2$ large and 20 cm thick optical table (Standa, Lithuania). The fully-automated setup is placed inside a separate room within the laboratory to decouple it from temperature fluctuations of the air-conditioning system. For trapping, we used a diode-pumped neodymium gadolinium vanadate ($\text{Nd}:\text{GdVO}_4$) infrared laser (2 W at $\lambda = 1064 \text{ nm}$, Smart Laser Systems, Berlin, Germany). The laser is linearly polarized, orthogonal to the optical table. The beam was kept 40 mm above the table and expanded in two steps to a final diameter of 7.8 mm such that the overfilling ratio was 1.3 (laser beam diameter divided by objective aperture diameter). The laser is initially expanded using a three-lens Galilean telescope enabling to change the expansion in a continuous fashion. To change the laser intensity, the polarization can be rotated by a $\lambda/2$ wave plate using a servo. A polarizing beam splitter determines the amount of transmitted light monitored by a quadrant photo-diode. The laser focus can be controlled dynamically relative to the imaging plane of the objective in three dimensions. For the axial direction, we can move a lens along the optical axis using a servo [11]. The lateral directions are controlled by a two-axis piezo tilt-mirror (NanoMTA2/2X, MadCity Labs, Madison, USA) placed in a conjugate plane with the back-focal plane of the objective by adjusting the subsequent mirrors in the light path [11].

Using a dichroic mirror, the laser is coupled into the self-made inverted microscope with a fixed objective that is used for trapping and imaging. The objective as well as the condenser are

infinity corrected CFI S Fluor 100 \times /0.7–1.3 oil objectives (Nikon, Japan).¹ The condenser objective can be centered above the trapping objective with two motors (Pico-motors 8353, New Focus, San Jose, USA). Otherwise, the condenser is designed as described in [6, 12] using a light emitting diode as a light source which is sufficient to image single microtubules with video-enhanced differential interference contrast (LED-DIC [12]). The sample is fixed with magnets (Supermagnete, Uster, Switzerland) and positioned with two piezo translation stages: (i) a long-range travel piezo-inertial drive (8 \times 8 \times 3.5 mm in x , y , and z , respectively; MS30,15, Mechanics Ag, Munich, Germany) and (ii) a nanopositioning stage (30 \times 30 \times 10 μ m, P-733.3DD, Physik Instrumente, Karlsruhe, Germany). We used non-imaging, back-focal plane detection in three dimensions [13] using a position sensitive diode (DL100-7PCBA3, Pacific Silicon Sensor, Westlake Village, USA). Calibration procedures were described previously [6, 14]. For imaging we used a CCD camera (Lu135M, Lumenera, Ottawa, Canada) attached to a variable zoom (0.7–4.9 \times , Sill Optics, Wendelstein, Germany). The whole setup is controlled via custom-written software programmed in LabVIEW (National Instruments, Austin, USA).

2.2. Stabilization of the laser

Laser stability with respect to pointing angle and intensity are crucial in order to achieve sub-nm resolution. We stabilized the laser intensity by adjusting the pumping laser diode current with a feedback circuit (nAmbition, Dresden, Germany) and measured a coefficient of variation of 0.003% over a period of 1000 s with 1 kHz sampling rate. This was a 10-fold improvement compared to no feedback. The laser had a pointing stability of 0.02 μ rad (standard deviation with 1 kHz sampling rate over 1000 s) for both x and y directions measured by pointing the laser directly onto a quadrant photo diode at \approx 50 cm distance. These pointing fluctuations led to laser displacements in the sample plane of \approx 0.01 nm.

2.3. Temperature feedback

The core elements of the temperature feedback are Pt100 temperature sensors attached to the objective and the condenser, heating foils wrapped around the objectives to give uniform heating, and a standard, software-based PID controller programmed in LabVIEW [Fig. 1(b)]. To ensure proper contact of the sensors and foils with the objectives, we used thermal conducting paste or glue. The heating foils (Minco SA, Aston, France) were connected to a power supply (E3631A Agilent, Santa Clara, USA) which communicated with the computer via an RS232 connection. The resistance of the sensors (class 1/3B) are measured in a three-wire configuration using standard electronics (PXT-10, Brodersen, Mülheim/Ruhr, Germany), digitized by a data acquisition card (NI PXI-6621, National Instruments, USA), and converted to temperature using the Callendar-Van Dusen equation. The temperature is measured every 0.25 s and the heat foil voltage updated accordingly. Additionally, we monitored the temperature of the microscope and the room. The sensors had an accuracy of \approx 0.15 $^{\circ}$ C and a sub-mK precision.

2.4. Sample preparation

The sample is made of two cleaned cover slips (18 \times 18 mm² and 22 \times 22 mm², No. 1.5, Corning, NY, USA) glued together by two pieces of double sticking tape. The separation caused by the tape forms a channel 18 \times 3 \times 0.1 mm³ in size with a volume of \approx 5 μ l. The channel was filled with an aqueous solution of 530 nm-diameter polystyrene microspheres (Polysciences,

¹Note that the objectives have a comparatively high transmission in the infrared of \approx 72% at 1064 nm but significant chromatic aberration leading to an infrared focal point several micrometers above the visible image plane. This was corrected for by the tube lens which did not affect our ability to image single microtubules by LED-DIC. Further note that current Nikon DIC sliders did not work in our counter-objective geometry. We had to revert to old models of DIC sliders.

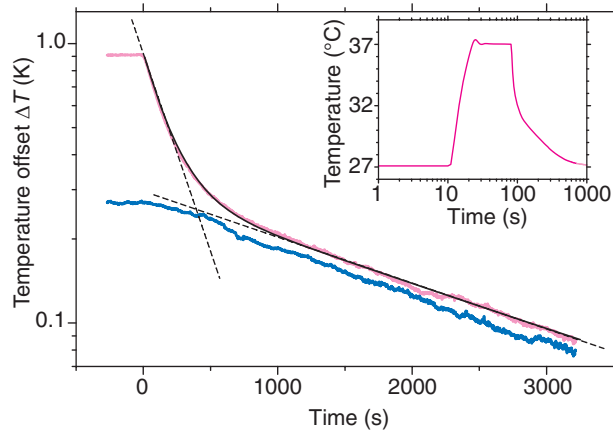


Fig. 2. Laser heating of the objective. Objective temperature deviation (—) above the final, equilibrium temperature as a function of time. At time zero the shutter was closed. The relaxation was fitted by a double exponential decay (—) that returned $\tau_o = 190$ s and $\tau_m = 2600$ s attributed to the objective and microscope, respectively. Guides to the eye (- -) indicate the fast and slow relaxation. Concurrently, the microscope temperature (—) decreased slowly. The laser power was ≈ 1.4 W at the back aperture of the objective, the starting temperature was 27.50°C , and the final temperature was 26.58°C . Inset: Objective temperature reached a 10°C higher set point temperature after ≈ 10 s using the temperature feedback. Return to the previous set point was slower.

Warrington, USA) containing 0.1 M KCl and sealed with nail polish. The salt screened the electrostatic repulsion and resulted in surface-immobilized microspheres [6].

3. Results

3.1. Significant laser heating and slow relaxation

How much does the laser heat the objective and how long does it take to equilibrate? To measure the amount of laser heating without the temperature feedback, we operated the optical tweezers at full power—nominally 2 W laser output reduced to ≈ 1.4 W at the back aperture of the objective—and let the system equilibrate over night. Then we closed the shutter and recorded the objective and microscope temperature as a function of time (Fig. 2). The objective temperature relaxation was well described by a double exponential fit. We attribute the short relaxation time, $\tau_o = 190$ s, to the objective and the long one, $\tau_m = 2600$ s, to the microscope since the slow relaxation approached the microscope temperature. Thus, when the shutter was closed for a long time, the optical tweezers needed at least two hours ($\approx 3\tau_m$) to thermally equilibrate once the laser was turned back on. With an overfilling ratio of 1.3, about 30% of the laser intensity was absorbed at the back aperture of the objective. Using an iris in front of the objective with the same aperture as the latter reduced the amount of objective heating by $\approx 30\%$ heating the iris instead. We did not use an iris because it conflicted with beam steering and relaxation times did not shorten when using the iris. To circumvent long equilibration times, we implemented temperature-controlled objectives that are heated a few degrees above room temperature. With the feedback, the heating foils compensate for the loss of laser heating when the laser is turned off maintaining the objectives at a constant temperature.

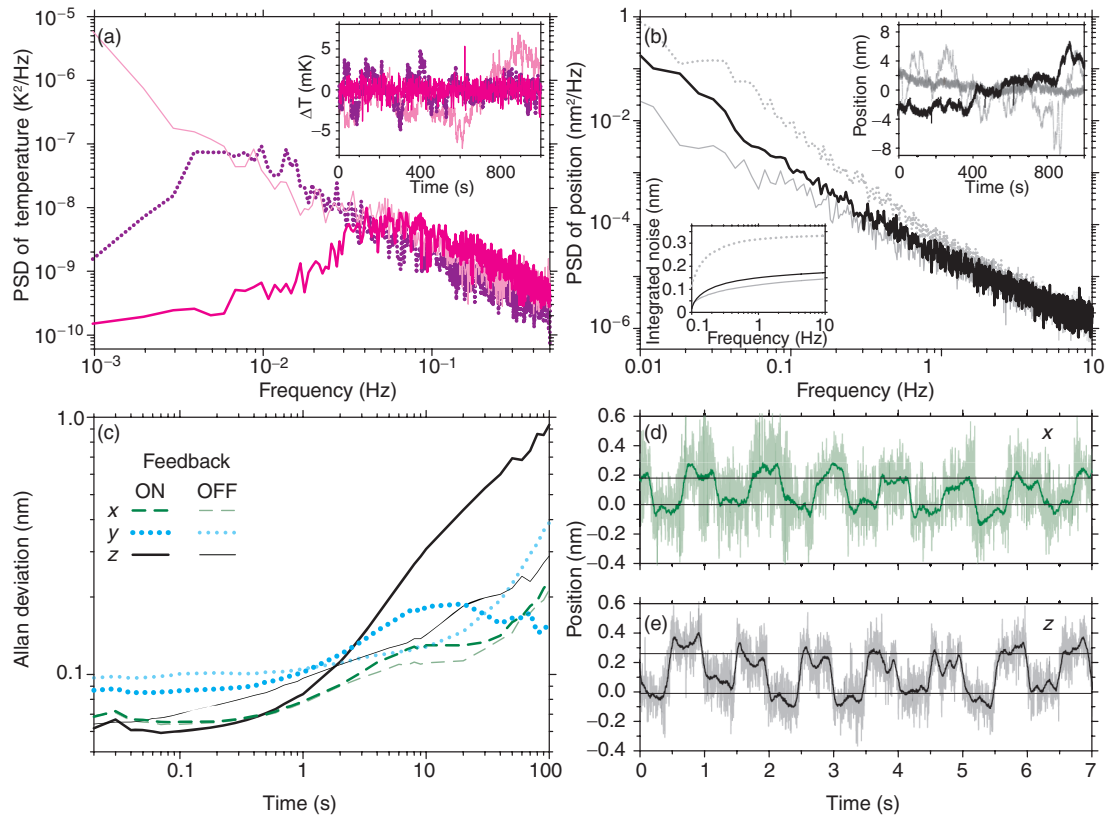


Fig. 3. Stability of objective temperature and immobilized-microsphere position. (a) Power spectral density (PSD) of the objective temperature for the feedback — OFF, ON with single-, — ON with double-heat-foil configuration. Inset: Deviation of the objective temperature from the mean as a function of time for the feedback. (b) PSD of the axial position for the three cases (— OFF, ON with single-, — ON with double-heat-foil configuration). All PSD curves are an average of 8 spectra. Upper inset: Deviation of the axial position from the mean as a function of time. Lower inset: Integrated positional noise as a function of frequency. (c) Allan deviation of position with the double-heat-foil configuration and without temperature feedback. (d,e) Steps of an immobilized microsphere created by moving the piezo translation stage with $\Delta x = 0.18$ nm in (d) and $\Delta z = 0.27$ nm in (e). Data were acquired with a sampling frequency of 10 kHz and are displayed with 10 Hz (200 Hz, shaded colors) bandwidth obtained by adjacent averaging.

3.2. Optimal temperature sensor and heating foil positions

The position of the temperature sensor and the heating foil played a crucial rule for the performance of the feedback. The shorter the distance between the sensor and the foil, the shorter the lag time of the feedback improving its bandwidth and performance (Fig. 3). For optimal heat compensation, the heating foil should ideally be placed where the laser is heating the objective most. However, this position is *a priori* unknown and might not be accessible due to the geometry of the objective. For example, unsuitable positions on our objective were the spring-loaded tip and the adjustment collar for the numerical aperture [see Fig. 1(b)]. We mounted one heating foil directly underneath the adjustment collar and one above it. One temperature sensor was placed above the upper heating foil as close as possible to the sample and one below the lower

one. We tested two feedback configurations: (i) usage of only the upper sensor controlling the lower heating foil (at a distance of ≈ 20 mm) with the upper heating foil turned off and (ii) both sensors controlling the heating foil next to them (≈ 3 mm spacing between sensors and foils). In the latter case, the temperature set point of the lower feedback was 0.25 K lower than for the upper one. This temperature gradient resembled the one created by the laser itself. The standard deviation of the temperature near the sample measured over 1000 s in steady conditions was 2.9, 1.5, and 0.9 mK for the feedback off, the feedback on with one and two operating heating foils, respectively [inset Fig. 3(a)]. The response times of the feedback were 32 and 8 s for the single- and double-heating-foil configuration, respectively [Fig. 3(a)]. Even though the double-heating-foil configuration performed better with respect to temperature stability and response time, the single-heating-foil configuration resulted in less axial movement of an immobilized microsphere with respect to changes in laser intensity (see Sect. 3.5).

3.3. *Single DNA base-pair resolution with temperature feedback*

To judge the performance of the temperature feedback with respect to the positional stability of the optical tweezers, we tracked immobilized microspheres. This is the most stringent test for the setup because it measures fluctuations of both the surface and the laser. The standard deviation of the axial position measured over 1000 s in steady conditions was 0.7, 2.9, and 2.4 nm for the feedback off, the feedback on with one and two operating heating foils, respectively [upper inset Fig. 3(b)]. Note that the good value without feedback was only reached after long equilibration times without any disturbance of the room, i.e. not practical every day conditions. The power spectral density (PSD) of the position revealed that the temperature feedback introduced additional noise in the axial direction for time periods longer than ≈ 1 s. The integrated noise [lower inset Fig. 3(b)] for 0.1–10 Hz was below one DNA base pair (0.34 nm—the spacing between subsequent nucleotides) with the double-heating-foil configuration performing nearly as good as without the feedback. Since the magnitude of the integrated noise critically depends on the lower frequency bound, we calculated the Allan deviation (Fig. 3(c), [15]) to get a measure of the noise level for all time periods. For periods longer than 1 s, the feedback (two-foil version) introduced additional axial noise compared to no feedback. For the lateral directions, results were comparable to, if not better than, the case without the feedback. Nevertheless, even for the axial direction single base-pair resolution was reached based on the Allan deviation for times shorter than ≈ 10 s. We directly tested this resolution by moving the stage in a stepwise manner [Fig. 3(d,e)]. In both lateral and axial directions, we could resolve steps smaller than a single base pair. Thus, the setup is capable of high-resolution measurements of DNA-protein interactions [2, 4] in a surface-coupled assay [16].

3.4. *Trap movement correlated with temperature changes*

Using the temperature feedback, we measured how much the laser focus moved upon temperature changes. We changed the set point temperature for both objectives in increments of 20 mK about every ≈ 300 s recording the microsphere position simultaneously (Fig. 4). Reversal of the steps also reversed the position of the microsphere. For example, the zero position for the axial direction was revisited to within ≈ 10 nm after ≈ 3000 s. For each step, positions were averaged after the transient response of the feedback and plotted against the temperature change (inset Fig. 4). Linear fits to the data resulted in 0.07, 0.05 and 1.0 nm/mK movement for x , y and z , respectively. The displacement sensitivity with respect to temperature changes was largest in the axial direction. This, we attributed to the thermal expansion of the objective: With the linear thermal expansion coefficient of brass, $19 \cdot 10^{-6} \text{ K}^{-1}$ multiplied by the size of the objective, 6 cm, we arrive at 1.14 nm/mK which is in good agreement with our measurements. Thus, the heating mainly expanded the trapping objective while all the other components of the optical

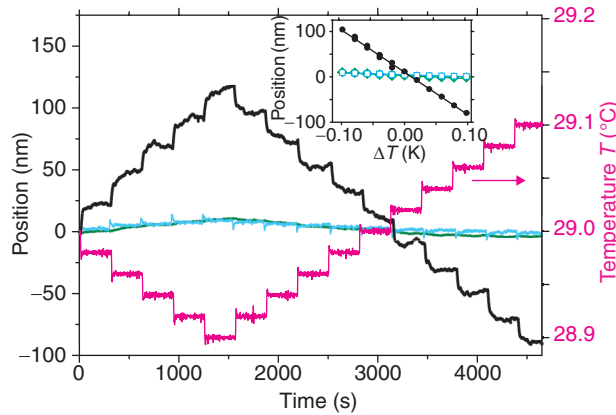


Fig. 4. (a) Displacement response of microsphere position (\blacktriangleleft x , \blacktriangleright y , and \blacktriangleup z ; left-hand axis) to 20 mK steps of the temperature set point (step duration: ≈ 300 s; \blacktriangle objective temperature T , right-hand axis). Inset: Microsphere position (\blacktriangleleft x , \blacktriangleright y , and \blacktriangleup z) as a function of temperature deviation.

tweezers remained stationary on the time scale of the experiment. The smaller drift in the lateral directions indicated that heating of the laser and the heating foils was uniform and did not lead to significant bending of the objective.

3.5. Feedback restores equilibrium fast

To study the effectiveness of the temperature feedback, we closed the shutter for different time intervals and measured how long the system needed to restore its initial state with and without the feedback (Fig. 5). The shutter was closed for various time periods (grey boxes). During the closure time, the laser did not heat the objective. Without the feedback [Fig. 5(c)] the temperature decreased depending on the duration of the closure. Surprisingly, even a closure as short as 5 s resulted in ≈ 20 nm axial movement. The re-equilibration time was ≈ 200 s. For the 100 s closure, the waiting time increased to more than 20 min with axial displacements of ≈ 300 nm. In contrast, using the feedback [Fig. 5(a,b)] the system re-equilibrated within ≈ 100 s independent of the closure time. Using the feedback with the single heating foil [Fig. 5(a)], the axial position changed by ≈ 50 nm at most. The drawback of this feedback was the increased positional noise with a slower response time compared to two heating foils. With two heating foils employed [Fig. 5(b)], the axial movements are comparable to the ones in the absence of the feedback, however, the time needed to re-equilibrate was much faster. The different behavior of the two feedback configurations we ascribed to the unknown heating profile of the laser. While the temperature was locally controlled by the feedback, the overall temperature distribution and thus the average temperature of the objective might be different when the laser or the foils heat the objective. The single-heating-foil configuration resulted in a thermal expansion comparable to the one from the laser, while the two-heating-foils version heated on average less than the laser resulting in a shrinking of the objective when the shutter was closed—a lowering of the focus with an apparent upward movement of the immobilized microsphere.

4. Discussion and conclusion

Our experiments have shown that laser heating of the objective can cause hundreds of nanometers of movements due to thermal expansion and that relaxation times are long. Both aspects

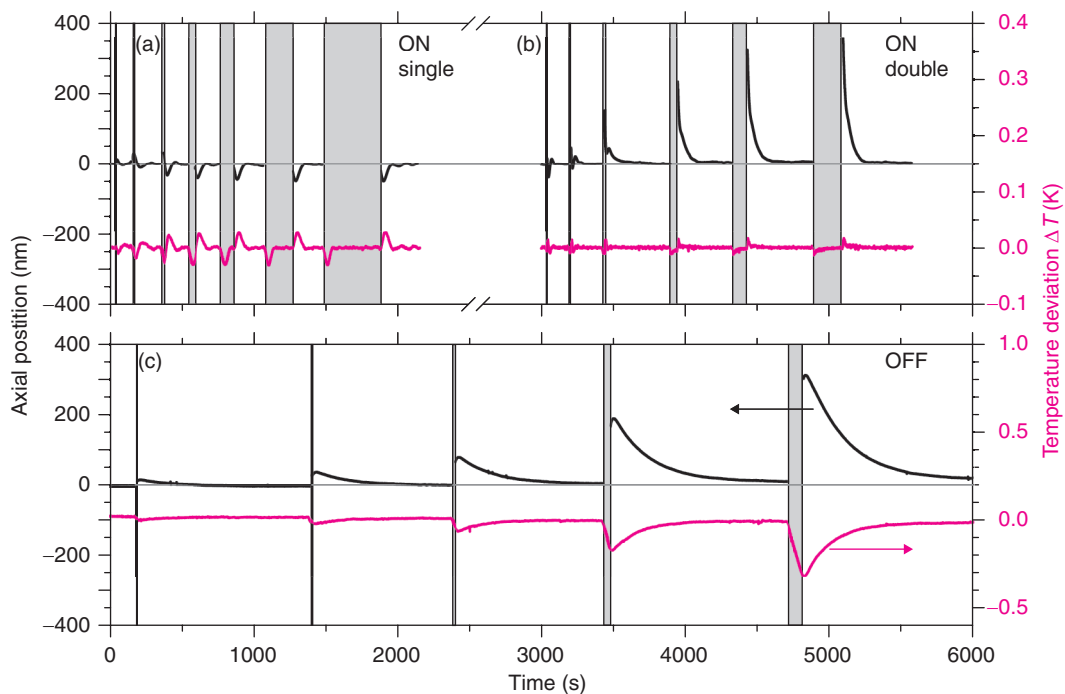


Fig. 5. Response to shutter closure. Axial microsphere position (—) and objective temperature deviation (—) from the equilibrium/set point temperature with temperature feedback ON [(a) single- and (b) double-heating-foil configuration] and OFF (c). Grey boxes represent closure periods (5, 10, 20, 50, 100, 200, and 400 s; not all long closure events are shown). During closures there was no laser reaching the position detector. Therefore, the microsphere position could not be measured leading to discontinuities in the trace.

are undesirable for sensitive, high-resolution, biophysical measurements. Therefore, we use the two-heat-foil configuration on an everyday basis. Remaining long-term drift we attribute—based on our temperature sensors throughout the laboratory—to the slow temperature cycle of the building, random heat sinks (e.g. opening of a door or the sleep-mode of a monitor), and the presence of extra heat sources in the room such as the human body. Compared to published [10] and commercially available objective heaters we achieved an improved temperature stability. This improvement we ascribe to the long-term stability of the Pt100 elements, the fast response time of the heating foils, the good thermal contact between sensors, foils and the objectives, and, last but not least, to the short distance between the sensors and the foils. Overall this led to the short lag times—i.e. the fast response of the feedback—and ultimately the millikelvin temperature stability.

The feedback improved relaxation times significantly to about 100 s, but introduced some extra positional noise. However, this noise was low enough that steps with a size smaller than a single DNA base-pair could still be resolved in both lateral and axial directions. Together, this improves the throughput of high-resolution experiments without the need of long equilibration times or sacrificing normal shutter usage. An important additional advantage of using the feedback is that experiments can be performed under *exactly* the same temperature condi-

tions independent of the time of the day or season. This is particularly important when studying biomolecules. Also, a fast increase in temperature is feasible (inset Fig. 2), e.g. to switch temperature-sensitive proteins. Other high-resolution microscopy techniques in particular ones that use high-power infrared lasers and/or scanning approaches, e.g. multi-photon excitation techniques or STED [17], should also benefit from a stabilized objective temperature.

Acknowledgments

We thank Fabian Czerwinski for sharing his MATLAB script to calculate the Allan deviation, and Marcus Jahnel and Marcel Ander for comments on the manuscript. The work was supported by the Deutsche Forschungsgemeinschaft (DFG, Emmy Noether Program) and the Technische Universität Dresden.